ELSEVIER

Polymer 40 (1999) 3829–3834

polymer

High-pressure DSC study of thermal transitions of a poly(ethylene terephthalate)/carbon dioxide system

Zhikai Zhong, Sixun Zheng, Yongli Mi*

Department of Chemical Engineering, The Hong Kong University of Science and Technology, Clear Water Bay, Kowloon, Hong Kong

Received 25 March 1998; received in revised form 30 June 1998; accepted 6 August 1998

Abstract

The thermal transitions of a poly(ethylene terephthalate)/carbon dioxide (PET/CO_2) system were investigated by using a differential scanning calorimeter accessorized with a high-pressure DSC cell. It was found that the glass transition temperature of PET decreases with an increase in the CO_2 pressure due to the plasticization effect, which is quite noticeable even at rather low CO_2 pressures. The sorbed CO_2 enhances the mobility of the chain segments and depresses the crystallization temperature of the PET. The CO_2-induced crystallization of PET at high pressure is attributed mainly to the plasticization effect, which causes a lower T_g than room temperature for PET, and hence crystallization of PET can occur at room temperature. The sorbed CO_2 was also found to be able to induce the crystallization of PET at temperatures lower than the glass transition temperature of PET. The results of high-pressure DSC were supported by measurements of wide-angle X-ray diffraction (WAXD).

Keywords: High-pressure DSC; PET; T_g

1. Introduction

In the past decades, the study of polymer–diluent systems has received extensive attention for environmental protection and industrial purposes, including the manufacture of foam plastics, packaging materials and membrane processes for gas separation [1–3]. It has been reported that high-pressure gases can be used to change polymer morphology and phase behaviour [4,5]. Recently, polymerization in supercritical fluids has been reported by several authors [6–9]. The small molecules dissolved in polymer matrices can induce complicated mass transfer behaviour, and, consequently, dissolution, diffusion, swelling and crystallization can occur. The resulting phenomena relate to the nature of the polymers and penetrants, the temperature, the pressure, the sample geometry, and the interaction between the polymer molecules and the small diluent molecules.

In the investigation of polymer/diluent systems, it is particularly important to study the plasticization and crystallization induced by gases or solvents [10–19]. Several studies of CO_2-induced crystallization have been reported for polycarbonate (PC) [15], poly(phenylene sulfide) [16], poly(aryl ether ether ketone) [17,18] and poly(ethylene terephthalate) (PET) [11,14,19]. However, the thermal properties from these studies were not in situ properties under high-pressure CO_2. The method adopted by these studies was to subject the polymer to a delay time between thermal characterization and pressurization, during which the polymer specimen was first enclosed in a high-pressure CO_2 chamber for a period of time to reach a sorption equilibrium, then the specimen was taken out of the chamber for measurement after the pressure was released. In our previous study, we reported the in situ DSC study of the T_g of a bisphenol A polycarbonate (PC)/CO_2 system and that the T_g of the system was depressed significantly by high pressure N_2 or CO_2 [20]. In this study, we present measurements of the in situ thermal transitions of PET under high-pressure CO_2 in order to understand the interaction of polymers with gas molecules and the mechanisms of plasticization and gas-induced crystallization. With an on-line high-pressure DSC cell mounted on a normal DSC apparatus, we can keep the pressure of CO_2 constant during DSC analysis. We were thus able to detect the in situ thermal transitions of PET, such as the glass transitions, crystallization and the melting process, and to monitor the variation of these transitions with CO_2 pressure.

* Corresponding author.

0032-3861/99/$ - see front matter
PII: S0032-3861(98)00594-1

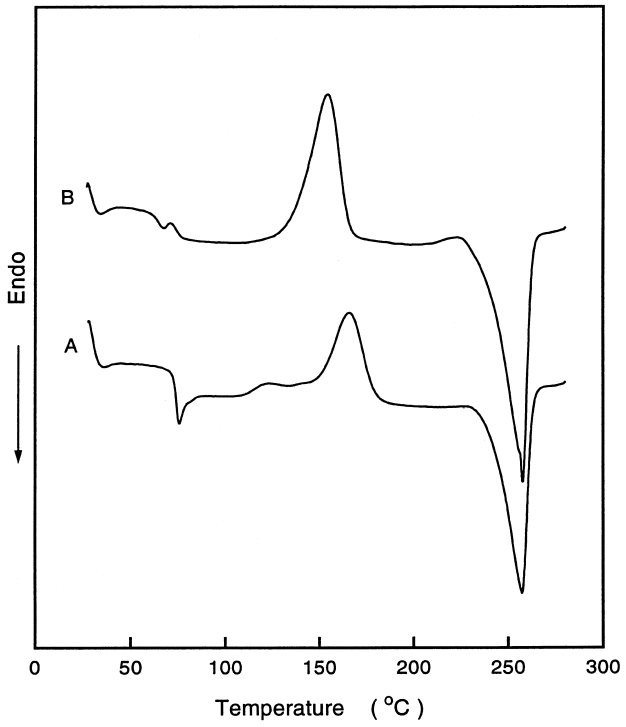

Fig. 1. DSC thermograms of (A) the 'as-received' PET pellet and (B) the PET film (quenched in liquid nitrogen).

2. Experimental method

2.1. Materials and preparation

The PET pellet (CAT# 138; $d = 1.385$) was obtained from Scientific Polymer Products, Inc., Ontario, NY, USA. The PET pellet became molten at 280°C after 5 min in a hot press. The molten PET was then pressed into a thin film about 200 μm thick. After keeping the thin film at 280°C for another 5 min, the PET was immersed into liquid nitrogen to obtain an amorphous PET film. The gas used in this study is high-purity ultra-dry CO_2, purchased from Hong Kong Town Gas Company.

2.2. Apparatus and methods

The measurements of the thermal properties of PET were conducted on a TA 2910 differential scanning calorimeter. A special accessory, a high-pressure DSC cell, was ordered from TA Instruments, Delaware, USA; this enables us to run DSC measurements under different gases at pressures up to 70 atm.

To start the high-pressure DSC measurement, the PET film was enclosed in the sample pan, and a small hole was pricked in the top of the pan to allow gas to contact the polymer enclosed in the sample pan during the measurement. The sample pan and reference empty pan were first put into the high-pressure DSC cell, then CO_2 was slowly dispersed into the cell in order to purge the air from the cell. After this operation, the CO_2 was pressurized to the desired level. The sample was exposed to this CO_2 environment for adequate time for sorption equilibrium to be achieved, and for the whole period the temperature of the cell was kept at room temperature (25°C). After that, the sample was heated to 280°C at a rate of 10°C min^{-1} and kept at 280°C for 1 min. Then the sample was cooled to 150°C at 5°C min^{-1}. During the measurement, the pressure of the CO_2 was kept constant in the cell. The glass transition temperature (T_g) was taken as that of the midpoint of the transition. The crystallization temperature (T_c) and the melting-point temperature (T_m) were taken as the minimum of the exothermic peak and the maximum of the endothermic peak, respectively.

Wide-angle X-ray diffraction (WAXD) patterns were determined with a Philips PW 1830 diffractometer with CuKα radiation, operating at 40 kV and 40 mA at room temperature. The angular scale and recorder reading (2θ) were calibrated to an accuracy of 0.05°.

3. Results and discussion

The PET film prepared in this work was transparent. The DSC thermogram of the PET film is shown in Fig. 1 (curve B). For comparison purposes, the DSC thermogram of the 'as-received' PET pellet is also presented in Fig. 1 (curve A). Some obvious differences between these two PET samples can be found in the figure. First, the PET pellet exhibits an ageing peak, which can be explained by an enthalpy relaxation mechanism. The PET film shows no ageing phenomenon because it was obtained by quenching. Secondly, the T_g and T_m of these two samples are almost the same (74°C and 257°C, respectively), whereas the T_c of the PET film is lower than that of the PET pellet by 11°C. Finally, the area difference between the endothermic melting peak and the exothermic crystallization peak for the PET film is 10.26 J g^{-1}, which is smaller than that for the PET pellet (19.29 J g^{-1}). Such an area difference for the PET film means that a completely amorphous PET was not obtained even by quenching the molten PET in liquid nitrogen. However, it is clear that the PET pellet has higher crystallinity than that of the quenched PET film.

According to the solution–diffusion mechanism, solution is a quick process, whereas diffusion is slower. The latter determines the time required for the sorption equilibrium to be reached. In our experiment, the DSC thermograms of the PET film exposed to CO_2 at 15 atm and equilibrated for 10 h and 21 h, respectively, were found identical. It was also found that the T_g, T_c and T_m of the PET film exposed to CO_2 for 10 h were same as those of PET film exposed to CO_2 for 21 h. The enthalpies related to crystallization and melting were also not significantly different between these two samples. Thus, in our opinion, 21 h is a sufficient time for sorption equilibrium for CO_2 in PET film at 25°C.

Figs. 2 and 3 show the DSC traces of the PET film at

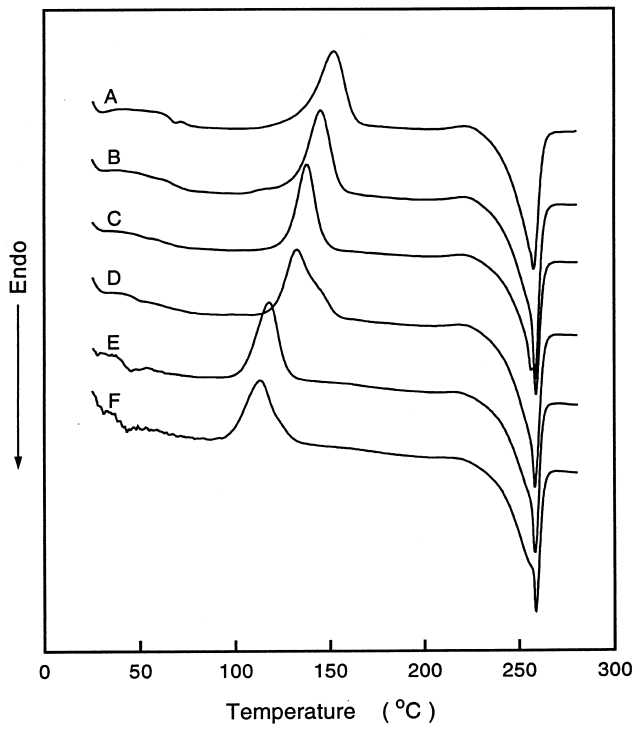

Fig. 2. DSC thermograms of the quenched PET film with exposure to CO_2 atmosphere for 21 h at (A) 0 atm; (B) 5 atm; (C) 10 atm; (D) 15 atm; (E) 25 atm; and (F) 30 atm.

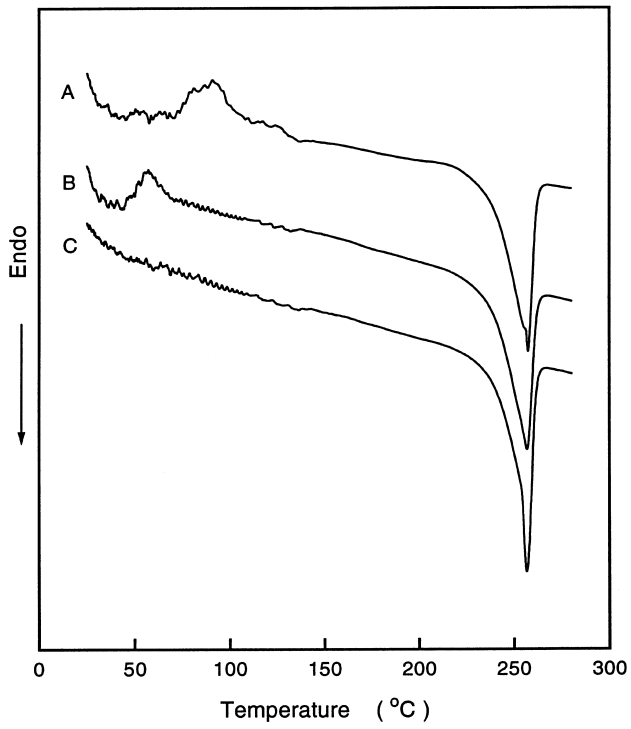

Fig. 3. DSC thermograms of the quenched PET film with exposure to CO_2 atmosphere at (A) 40 atm for 21 h; (B) 50 atm for 21 h; and (C) 50 atm for 45 h.

different pressures in CO_2 atmosphere. In Fig. 2, all the DSC traces clearly exhibit glass transition, crystallization exothermic peak and melting endothermic peak. Although the DSC traces of the PET film exposed to CO_2 pressure higher than 25 atm show some turbulence at the initial parts of the diagram, this turbulence does not affect the determination of T_g for these samples. Based on Figs 2 and 3, several interesting results can be found. Firstly, the T_g of the PET film decreases with increasing CO_2 pressure, and, for the samples exposed to the CO_2 atmosphere with a pressure higher than 30 atm, no glass transition can be detected in the experimental conditions. Secondly, the T_c of the PET film also decreases with increasing CO_2 pressure. Thirdly, the T_m of these samples looks invariant with changing pressure. Compared with the sample exposed to 0 atm air, the PET film exposed to 0 atm CO_2 shows lower T_g and T_c but the same T_m. (It should be noted that the pressure value used in this work is the gauge pressure of the pressure DSC cell during the measurement. Therefore, 0 atm is equivalent to 1 atm absolute pressure.)

For the purpose of quantitative analysis, the results obtained from Figs 2 and 3 are summarized in Table 1 and Fig. 4. It can be seen that the T_g of the PET film decreases from 74°C at 0 atm air to 72°C at 0 atm CO_2, to 48°C at 15 atm CO_2, and then to 37°C at 30 atm CO_2. The T_g reduction of PET in a CO_2 environment was also observed by Chiou et al. [11], who found that the T_g of PET decreases from 74°C to 52°C at 20 atm. The greater reduction of T_g found in our experiments than in Chiou's is probably due to the difference in experimental methodology. Since Chiou et al. carried out their DSC experiment after releasing the CO_2 pressure, they could not obtain in situ properties of PET in

Table 1
Thermal properties of PET measured by high-pressure DSC (ND: not detected)

	T_g (°C)	T_c (°C)	ΔH_c (J g^{-1})	T_m (°C)	ΔH_f (J g^{-1})	X_c (%)
0 atm, in air	74	154	43.2	258	53.5	7.3
0 atm, in CO_2	72	152	43.9	258	57.8	9.9
5 atm, in CO_2	67	145	41.5	259	59.6	12.9
10 atm, in CO_2	51	138	39.8	259	59.3	13.9
15 atm, in CO_2	47	130	37.8	258	57.5	14.1
25 atm, in CO_2	41	118	32.8	258	54.6	15.5
30 atm, in CO_2	37	113	31.1	259	52.6	15.4
40 atm, in CO_2	ND	91	23.9	258	51.9	20.0
50 atm, in CO_2	ND	57	6.2	257	50.4	31.6

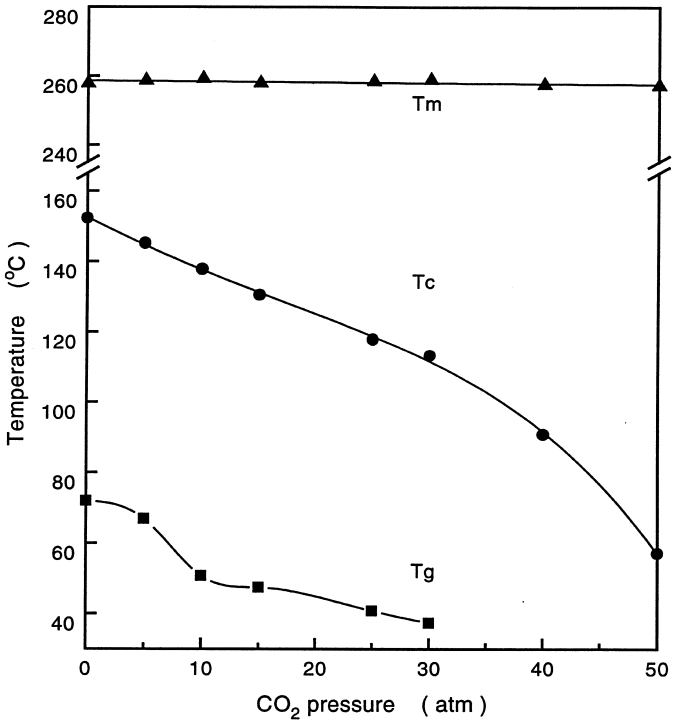

Fig. 4. The pressure dependence of the glass transition temperature, T_g, crystallization temperature, T_c, and melting temperature, T_m, of PET as a function of CO_2 pressure.

CO_2 and, as a result, they obtained a somewhat smaller T_g reduction.

The reduction of T_g is known as the plasticization effect of CO_2. The higher the CO_2 pressure and hence the more sorbed CO_2 in the polymer, the lower the T_g of the PET film. Because the dominant components of air are nitrogen and oxygen, and because the solubility of N_2 and O_2 in PET is lower, the T_g of the PET film exposed to 0 atm CO_2 is lower than that exposed to 0 atm air. For higher CO_2 pressures than 30 atm, the T_g of the PET film became lower than the starting temperature of our experiments; hence, the T_g cannot be detected. The pressure DSC cell produced by TA Instruments does not have a cooling system. As a result, we were unable to determine thermal transitions below room temperature. Mensitieri et al. [19] reported that only at high pressures is CO_2 able to plasticize the PET and consequently to promote its crystallization. However, according to our results in this study, CO_2 can plasticize PET even at rather low pressures (cf Fig. 4). It should be pointed out that the high-pressure gas affects the T_g of the polymer in two ways; namely, the dissolved gas tends to lower the T_g and the hydrostatic pressure exerted by the gas tends to raise the T_g. In our experimental conditions, it is obvious that the decrease of T_g due to the absorbed CO_2 is dominant. On the other hand, it is reasonable to think that the actual reduction of T_g due to the plasticization effect could be stronger than that shown in Table 1 and Fig. 4.

In Fig. 4, it can be seen that the T_m of the PET film remains almost constant at about 258°C at CO_2 pressures up to 50 atm. We believe that the absorbed CO_2 mainly stays in the amorphous region of the PET, whereas no gas molecules penetrate into the crystal region. As a result, chain mobility in the PET crystalline region is not enhanced by the sorbed gas. Another reason for the invariancy of T_m of PET relative to the CO_2 pressure is that T_m reflects the degree of perfection of the polymer crystallites. Since high pressure CO_2 does not result in imperfection of PET crystallites, the T_m will not be depressed. From the thermodynamic point of view, T_m should increase with increasing hydrostatic pressure. However, in order to observe such an increase, the required pressure should be high enough, say beyond 1000 atm. Within the pressure range of this study (0–50 atm) the pressure effect on T_m cannot be detected. It should also be noticed that the amount of CO_2 sorbed in PET at elevated temperatures becomes progressively smaller, which makes it difficult to study the effect of high pressure gas on the T_m of PET.

It is interesting to see that the T_c of the PET film decreases remarkably with the increase of CO_2 pressure. In the low-pressure range the T_c decreases linearly from 154°C at 0 atm air to 152°C at 0 atm CO_2, to 130°C at 15 atm CO_2, and to 113°C at 30 atm CO_2. Beyond 30 atm, the T_c decreases sharply to 91°C and 57°C at 40 atm and 50 atm, respectively. This phenomenon indicates that crystallization of PET becomes progressively easier with increasing CO_2 pressure. The reduction of T_c corresponds to the reduction of T_g, since lowering T_g enhances the mobility of the PET chain, and hence the transformation of the amorphous phase of PET to

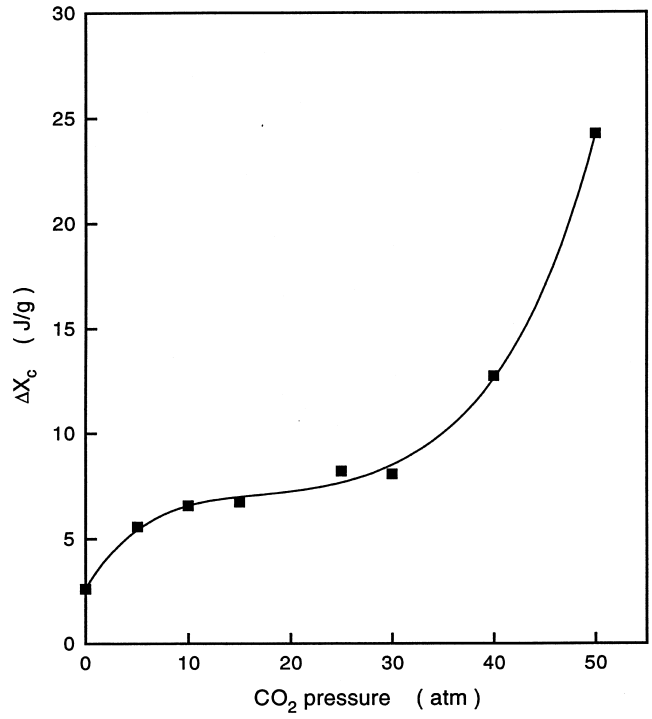

Fig. 5. The pressure dependence of ΔX_c as a function of CO_2 pressure.

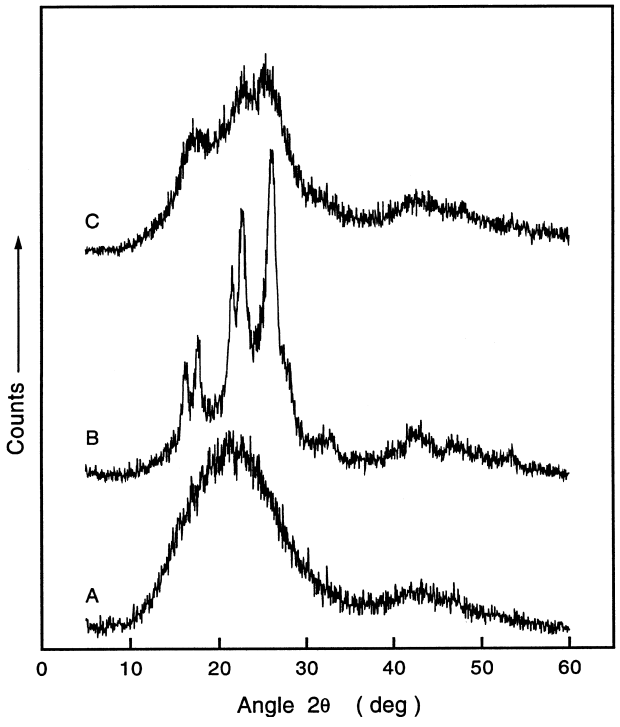

Fig. 6. X-ray diffraction patterns of (A) the quenched PET film without treatment; (B) the quenched PET film crystallized from a molten state under 15 atm CO_2 atmosphere; and (C) the quenched PET film exposed to 50 atm CO_2 atmosphere for 21 h at room temperature.

a lower free energy crystalline structure is kinetically favoured. The crystallization of PET prior to heating can be seen clearly from Fig. 3, in which a small crystallization exothermic peak can be found for the PET film exposed to 50 atm CO_2 for 21 h (curve B), whereas no obvious crystallization exothermic peak can be found for the samples exposed to 50 atm CO_2 for 45 h (curve C); this suggests that crystallization has already taken place under CO_2 at 50 atm and at experimental temperatures.

The crystallinity of PET can be calculated using the following equation:

$$X_c = (\Delta H_f - \Delta H_c)/\Delta H_f^0 \quad (1)$$

where X_c is the percentage of crystallinity, ΔH_f and ΔH_c are the heats of fusion and crystallization of PET, respectively, and $\Delta H_f^0 = 140\ J\ g^{-1}$ is the heat of fusion of 100% crystalline PET [21]. The calculated results are listed in Table 1. The crystallinity difference, ΔX_c, which can be used to characterize the crystalline extent of the PET film at room temperature during exposure to CO_2, is defined as:

$$\Delta X_c = (X_c)_{CO_2} - (X_c)_{air} \quad (2)$$

where $(X_c)_{CO_2}$ and $(X_c)_{air}$ are the crystallinity of the PET film in CO_2 and in 0 atm air, respectively. In Fig. 5, ΔX_c is plotted against CO_2 pressure. It can be seen that, at first, ΔX_c increases quickly with CO_2 pressure, then levels off at about 10 atm. At pressures beyond 30 atm, ΔX_c increases sharply again. The non-zero of ΔX_c at 0 atm indicates that CO_2 can induce crystallization of PET even in normal CO_2 atmosphere (0 atm gauge pressure) and at

room temperature. Keeping in mind that ΔX_c characterizes the crystalline ability of the PET in the CO_2 environment at room temperature, the crystallization of PET at low pressure of CO_2 cannot, in our opinion, be attributed to the T_g depression, because the T_g of these samples is much higher than room temperature (1). It is probably related to interaction between CO_2 and PET macromolecules which causes an ordered structure of the PET chain. Further studies are needed in order to understand more fully the mechanism of this type of CO_2-induced crystallization. It can be further seen that this behaviour is sensitive to the CO_2 content (related to CO_2 pressure) in the PET, and becomes more and more significant with increasing CO_2 pressure. When the pressure is higher than 30 atm, the CO_2-induced crystallization due to the plasticization effect is dominant since the T_g of the sample is lower than room temperature and the PET can crystallize significantly at room temperature; thus ΔX_c increases sharply.

Furthermore, WAXD experiments were performed and the X-ray diffraction patterns of different PET films are shown in Fig. 6. The untreated PET film exhibits a broad peak (curve A), which indicates that the crystallinity in this sample is very low and cannot be detected in WAXD experiments. In fact, the sample has a crystallinity of only 7.3%, from the DSC measurement. However, the PET film, which was exposed to 15 atm CO_2 for 21 h, then heated to 280°C and cooled to 150°C, presents obvious crystalline characteristics and shows five sharp peaks in the X-ray diffraction pattern (curve B), because it has a crystallinity of 40.2%, from the DSC result. As for the PET films which were exposed to 50 atm CO_2 for 21 h at room temperature, some obvious crystalline characteristics can also be found in the X-ray diffraction diagram (curve C). This result also confirms that CO_2 can induce crystallization of PET at room temperature.

4. Conclusions

The results presented here show that CO_2 can plasticize PET at both low and high pressures. The crystallization temperature decreases with the increase of CO_2 pressure whereas the melting temperature remains constant. It was found that CO_2 can induce the crystallization of PET at temperatures lower than the T_g of PET. At lower pressures the induced crystallization cannot be attributed to the reduction of T_g, but at higher pressures plasticization of PET is a dominant effect in CO_2-induced crystallization. WAXD analysis also shows that CO_2 can induce crystallization of PET.

Acknowledgements

This work was supported by RGC, the Earmarked Grant for Research (No. 581/94E), HKUST 96/97.

References

[1] Gorski RA, Ramsey RB, Dishart KT. J Cell Plast 1986;22:21.
[2] Koros WJ, editor. Barrier polymer and structures. Washington, DC: American Chemical Society, 1990.
[3] Mi Y, Zhou S, Stern SA. Macromolecules 1991;24:2361.
[4] Dixon DJ, Luna-Barcenas G, Johnston KP. Polymer 1994;35:3998.
[5] Handa YP, Roovers J, Wang F. Macromolecules 1994;27:5511.
[6] DeSimone JM, Guan Z, Elsbernd CS. Science 1992;257:945.
[7] Combes JR, Guan Z, DeSimone JM. Macromolecules 1994;27:865.
[8] Watkins JJ, McCarthy TJ. Macromolecules 1994;27:4845.
[9] DeSimone JM, Maury EE, Menceloglu YZ, McClain JB, Romack TJ, Combes JR. Science 1994;265:356.
[10] Chiou JS, Barlow JW, Paul DR. J Appl Polym Sci 1985;30:2633.
[11] Chiou JS, Barlow JW, Paul DR. J Appl Polym Sci 1985;30:3911.
[12] Chiou JS, Maeda Y, Paul DR. J Appl Polym Sci 1985;30:4019.
[13] Kamiya Y, Mizoguchi K, Natio Y, Hirose T. J Polym Sci Polym Phys Ed 1986;24:535.
[14] Mizoguchi K, Hirose T, Naito Y, Kamiya Y. Polymer 1987;28:1298.
[15] Beckman E, Porter RS. J Polym Sci Polym Phys Ed 1987;25:1511.
[16] Schultze JD, Bohning M, Springer J. Makromol Chem 1993;194:339.
[17] Handa YP, Capowski S, O'Neill M. Thermochim Acta 1993;226:177.
[18] Handa YP, Kruus P, O'Neill M. J Polym Sci Polym Phys Ed 1996;34:2635.
[19] Mensitieri G, Del Nobile MA, Guerra G, Apicella A, Al Ghatta H. Polym Eng Sci 1995;35:506.
[20] Mi Y, Zheng S. Polymer 1998;39:3709.
[21] Wunderlich B. Polym Eng Sci 1978;18:431.